fluids

MDPI

Article

Numerical Study of Large-Scale Fire in Makkah's King Abdulaziz Road Tunnel

Kamel Guedri [1,2,*], Abdullah A. Abdoon [1], Omar S. Bagabar [1], Mowffaq Oreijah [1], Abdessattar Bouzid [1] and Shadi M. Munshi [1]

[1] Mechanical Engineering Department, College of Engineering and Islamic Architecture, Umm Al-Qura University, Makkah 21955, Saudi Arabia; bin.abdoon83@gmail.com (A.A.A.); omarbajaber4@gmail.com (O.S.B.); mmoreijah@uqu.edu.sa (M.O.); abdes.bouzid@gmail.com (A.B.); smmunshi@uqu.edu.sa (S.M.M.)

[2] UR: MEER, Faculty of Sciences of Gafsa, University of Gafsa, Gafsa 2112, Tunisia

* Correspondence: kmguedri@uqu.edu.sa; Tel.: +966-563-884-798

Abstract: Tunnel fires are one of the most dangerous catastrophic events that endanger human life. They cause damage to infrastructure because of the limited space in the tunnel, lack of escape facilities, and difficulty that intervention forces have in reaching the fire position, especially in highly crowded areas, such as Makkah in the Hajj season. Unfortunately, performing experimental tests on tunnel fire safety is particularly challenging because of the prohibitive cost, limited possibilities, and losses that these tests can cause. Therefore, large-scale modeling, using fire dynamic simulation, is one of the best techniques used to limit these costs and losses. In the present work, a fire scenario in the Makkah's King Abdulaziz Road tunnel was analyzed using the Fire Dynamics Simulator (FDS). The effects of the heat released per unit area, soot yield, and CO yield on the gas temperature, radiation, concentrations of the oxygen and combustion products CO and CO_2, and air velocity were examined. The results showed that the radiation increased with the heat released per unit area and the soot yield affected all parameters, except the oxygen concentration and air velocity. The CO yield significantly affects CO concentration, and its influence on the other studied parameters is negligible. Moreover, based on the validation part, the results proved that FDS have limitations in tunnel fires, which impact the smoke layer calculation at the upstream zone of the fire. Therefore, the users or researchers should carefully be concerned about these weaknesses when using FDS to simulate tunnel fires. Further comprehensive research is crucial, as tunnel fires have severe impacts on various aspects of people's lives.

Keywords: tunnel fire; heat release rate; gas temperature; CO yield; soot yield; air velocity

Citation: Guedri, K.; Abdoon, A.A.; Bagabar, O.S.; Oreijah, M.; Bouzid, A.; Munshi, S.M. Numerical Study of Large-Scale Fire in Makkah's King Abdulaziz Road Tunnel. *Fluids* **2022**, *7*, 5. https://doi.org/10.3390/fluids7010005

Academic Editor: D. Andrew S. Rees

Received: 20 November 2021
Accepted: 17 December 2021
Published: 22 December 2021

1. Introduction

The flame is spread very quickly, so that the source of fire changed from one point to another. The spread of flame in a solid surface, such as walls or combustible materials, is considered a significant issue that increases the propagation of fire and raises the heat. For example, if a fire starts in an object that is close to the wall in a tunnel, the first item ignited a tunnel fire and the wall enclosed with combustible substance. The wall lining could burn and spread the fire very quickly, so that the fire source will transfer to one or more sources [1–5]. Most fire deaths do not occur because of burns, but because of smoke inhalation. When a fire reaches the growth stage, the smoke loaded with toxic gases spreads in the space completely and rapidly, which prevents people from accessing emergency exits.

Fire characteristics in tunnels differ from that in open fires in two ways: heat feedback of the surrounding environment and effectiveness of natural ventilation on the fire. Crucial factors that affect the characteristics of fires in tunnels are fuel and ventilation control [3–8]. A fuel-controlled condition means that the amount of air is sufficient to sustain the fire during the entire combustion process, whereas a ventilation-controlled situation means that

there is a lack of air during the combustion process. In addition, there is a difference between ventilation-controlled and fuel-controlled systems. The fire is ventilation controlled if the volumetric airflow rate, compared with the heat release rate (HRR) when the fire is low. Conversely, the fire is fuel controlled if the volumetric airflow rate, compared with the HRR when the fire is high [3–8].

The tunnel is a long and a narrow building, created underground, and the major problem in the tunnels is the safety of the occurrence of fires inside it. In recent years, many incidents occurred inside the tunnels and has laid claimed to disasters [3–6]. During last recent years, there have been several serious tunnel fires. The Baku underground railway system (Azerbaijan) in 1995, Channel Tunnel (France) in 1996, Monte Bianco tunnel (Italy) in 1999, and Fréjus road tunnel (Italy) in 2005 are some of the most serious tunnel disasters to date. Therefore, worldwide interest has been concentrated on the important aspects of tunnel safety. Consequently, new international safety regulations and standards have been proposed to reduce tunnel fire catastrophes. However, establishment of these regulations and standards require modeling techniques to simulate tunnel fires. The Fire Dynamics Simulator (FDS) is a computational fluid dynamics (CFD) software program, developed by the US National Institute of Standards and Technology (NIST) in 2000, that is used for fire flow simulation. It has been used to solve large variations in fire scenarios numerically, based on the Navier–Stokes equation. CFD describes the fire flow, smoke spread, heat flux, and temperature transit from fire [3–23].

Ingason, et al. [23] achieved 4 large-scale experiments in an empty tunnel in Norway. They measured temperature, CO and CO_2 concentrations, air velocities, radiation, and smoke progress.

Recently, a fire in a horseshoe-shaped tunnel has been modeled by Gao et al. [6] using the Fire Dynamics Simulator (FDS). The tunnel's ceiling was constructed by concrete. To ameliorate the accuracy of the model, modified equations have been suggested for maximum smoke temperature rise beneath the ceiling and longitudinal temperature decay. Therefore, the calculations prove to have a good agreement between experimental and numerical results.

To examine the influence of vehicular blocking scene on the smoke spread in the longitudinal ventilated tunnel fire, 30 simulation conditions were carried out by Lu et al. [11]. Their calculations proved that the maximum temperature and smoke spread was significantly affected by the blockage area ratio.

More Recently, in 2021, Xu et al. [4] discussed numerous full-scale analyses of a horseshoe-shaped tunnel structure in tunnel fires. Their results, using FDS, proved that there are some differences between the transverse temperature distribution of the near field and the far-field zone.

In the same year, Li et al. [3] used the Fire Dynamics Simulator (FDS) to simulate one-dimensional horizontal diffusion stag. They study the longitudinal distribution of temperature rise and CO concentration in tunnel fires with one opening portal. They concluded that, without ventilation, the temperature rises and CO concentration decays. Moreover, Taher Halawa and Hesham Safwa [5] studied the influence of presenting solid walls at the ceiling of a tunnel on reducing spread of smoke. All FDS' scenarios show that the introduction of solid obstacles decreases the lengths of smoke spread.

Tunnel fire disasters are less frequent than open fire accidents, but they are more destructive. The impact of a tunnel fire is intense and extremely dangerous to human life, owing to the limited space of the tunnel, lack of escape facilities, and difficulty that intervention forces have in arriving at the fire position. In addition, it causes damage to the infrastructure.

According to the Holy Makkah Municipality, there are 60 tunnels in Makkah (Saudi Arabia) and the holy sites: 50 for cars and 10 for pedestrians. Makkah itself has 40 tunnels for cars and four pedestrian tunnels. The other tunnels are in the holy sites: 10 for cars and 6 for pedestrians [16].

The vast number of tunnels and the enormous number of people, particularly during the Hajj season in Makkah and the holy sites, increase the hazards of tunnel fires that

endanger human life. For these reasons, tunnel fire effects must be studied, in order to reduce the hazards of fire in these tunnels and preserve human life and property. Therefore, in the present work, a parametric study of a fire simulation in the Makkah's King Abdulaziz road tunnel was conducted. The study is especially for this tunnel, owing to its high crowding during the Hajj season.

2. Methods

FDS (version 6.7.7) was used in this study. The FDS is based on Navier–Stokes equations, which are a series of partial differential equations used to describe the motion of a fluid. The conservation of mass, species, momentum, and energy equations can be found elsewhere [5–15].

FDS has been developed to study fundamental fire dynamics and combustion to provide a protected and secure tool against fire in residential and industrial constructions. It can be used to simulate and study boundary conditions, low-speed heat and smoke transfer, thermal radiation, flame spread, and fire suppression by sprinklers, as well as combustion, pyrolysis, and hydrodynamic models. FDS has been largely verified for different cases of tunnel fires; therefore, a parametric study of fire simulation in the Makkah King Abdulaziz Road Tunnel was conducted. The effects of the heat release rate per unit area (HRRPUA), soot yield, combustion heat, and length of the tunnel on the gas temperature, radiation, concentrations of the combustion products CO and CO_2, air velocity, and flame lengths were analyzed using the FDS [17–24].

2.1. Heat Feedback

The total radiation flux that affects the tunnel' fire heat feedback is expressed as (Figure 1) [14,15].

$$\dot{q}'' = \left(\dot{q}''_f + \dot{q}''_g + \dot{q}''_w + \dot{q}''_{rr}\right) \times \frac{\Delta H_{c,eff}}{T_s} \quad (1)$$

Here, $\dot{q}''_f$ is the radiation of the flame, $\dot{q}''_g$ is the radiation of hot smoke gasses, $\dot{q}''_w$ is the radiation of surrounding geometry, $\dot{q}''_{rr}$ is the backward radiation of the fuel surface, $\Delta H_{c,eff}$ is the combustion efficient heat, and T_s is the fire surface temperature.

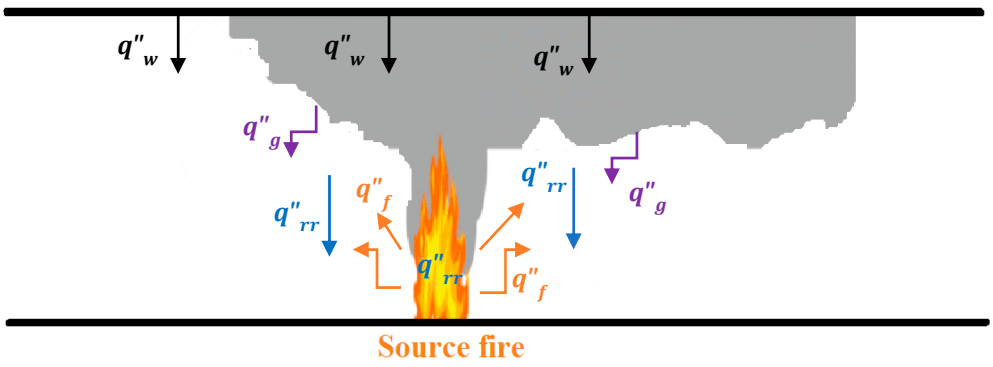

Figure 1. Balance of radiation heat transfer.

The radiation of the hot smoke gasses, illustrated in Equation (1), can be determined using:

$$\dot{q}''_g = F_g \in_g \sigma T_g^4 \quad (2)$$

and the radiation of the surrounding geometry:

$$\dot{q}''_w = F_w \in_w \sigma T_w^4 \quad (3)$$

Here, F is the view factor, ϵ is flame emissivity, σ is the Stefan–Boltzmann constant, and ΔT is the temperature difference between the object and surroundings.

Equations (1)–(3) describe the heat radiation, but there are heat losses through the walls resulting from heat conduction. To describe the heat conduction through the walls, the following Fourier's law is applied:

$$\boldsymbol{q} = -\kappa \boldsymbol{\nabla} T \tag{4}$$

Here, $\boldsymbol{q}$ is the heat flux, κ is the thermal conductivity, and $\boldsymbol{\nabla} T$ is the temperature gradient.

Equation (4) shows that κ (thermal conductivity) is a critical variable in the equation. Thermal conductivity describes the ability of a material to transfer heat. Table 1 shows the thermal conductivity of concrete and steel [14], which are the major components in tunnel construction.

Table 1. Thermal conductivity of tunnel construction.

Material	Thermal Conductivity [W/mK]
Concrete	0.8
Steel	50.2

2.2. Gas Temperature

The integrity of the tunnel structure is extremely reliant on the gas temperature, which can be used to predict heat exposure, fire detection time, and fire spread. The maximum ceiling gas temperature can be used to study the resistance of different tunnel's materials to prolonged temperature. It can be expressed as [14,15]:

$$T_{max} = \begin{cases} \dfrac{\dot{Q}^{\frac{2}{3}}}{17.5 H_{ef}^{\frac{5}{3}}}, V' \leq 0.19 \\ \dfrac{\dot{Q}}{u_0 b_{fo}^{\frac{1}{3}} H_{ef}^{\frac{5}{3}}}, V' > 0.19 \end{cases} \tag{5}$$

In this equation:

$$V' = \frac{u_0}{w^*} \tag{6}$$

$$w^* = \frac{g\dot{Q}}{b_{fo}\rho_0 c_p T_o} \tag{7}$$

Here, V' is the dimensionless ventilation velocity, w^* is the characteristic plume velocity, b_{fo} is the diameter of the fire, and H_{ef} is the effective height from the fire to the ceiling.

3. Results

3.1. Validation

The Runehamar Tunnel is 1600 m long, 6 m high, 9 m wide, and has a cross-sectional area of approximately 47 m^2. It has an oval shape with a slope varying between 1% and 3% [14]. In this section, the T4 test of Sweden's SP Technical Research Institute has been selected for validation [14]. It was preferred to validate the current study. The gas temperature, gas concentrations, radiation fluxes and air velocity were simulated at the different locations. Several previous studies have chosen the same test [1,2,14,17].

In our simulation, while the height and the wide of Runehamar tunnel were maintained, its length was cut 117 m upstream from the fire source, and, instead of an opening, a vent was placed in its place. Therefore, the simulated tunnel was 680 m length, 6 m high, and 9 m wide. In addition, its real oval shape was simplified to a rectangular one. In the full-scale experiment test T4 of [14], 600 corrugated paper cartons with interiors (600 mm × 400 mm × 500 mm), 15% of total mass of unexpanded polystyrene cups (18,000 cups), 40 wood pallets (1200 × 1000 × 150 mm), and 10 m^2 polyester tarpaulin have been considered. In our simulations, the fire was situated at 1037 m from the eastern portal

HGV trailer, with a surface of 30 m^2 and height of 3.3 m above the ground. It is positioned 1 m above the road surface [15]. The material properties used to simulate the fire are listed in Table 2 [14]. The results are obtained as outline sections of temperature, heat release, and velocity along the tunnel for the specified fire scenario, during 1200 s.

Table 2. Original input parameters for the combustion model.

Fuel	Diesel
Soot yield	0.046
Heat of combustion (kJ/kg)	21.05
CO yield	0.0145
HRRPUA (kW)	2214

FDS software cannot establish the circular ceiling surface, so its surface is transformed into approximate rectangular surface using a step-rectangular meshes (Figure 2) [19]. On other hand, grid scale is one of the main variables affecting the performance of numerical simulation. It is always a struggle to find the right grid cell size. In the FDS user guide, there are some guidelines, especially describing fire's dimensionless diameter. The mesh lengths depend on the variables of interest. Smaller fires will require finer meshes than larger fires. If a simulation case is used, the non-dimensional expression D^*/dx is used, where dx is the size for the grid and D^* is the dimensionless diameter, as expressed in the following words:

$$D^* = \left(\frac{\dot{Q}}{\rho_\infty C_p T_\infty \sqrt{g}} \right)^{\frac{2}{5}} \quad (8)$$

The value of D^*/dx is proposed to be between 4 and 16 [17–19], where a high number represents a fine grid, and a low number represents a coarse grid size. In this simulation, by using experimental properties of air, D^* will be 5.14. Using a grid size dx = 0.5 m, the corresponding D^*/dx will be 10.28, which is within the requirements [17–19]. Grid sensitivity analysis must be performed to determine that the grid resolution is accurate, and that the solution has reached convergence. Repetition of the grid cell size and comparison of the results were used in this study.

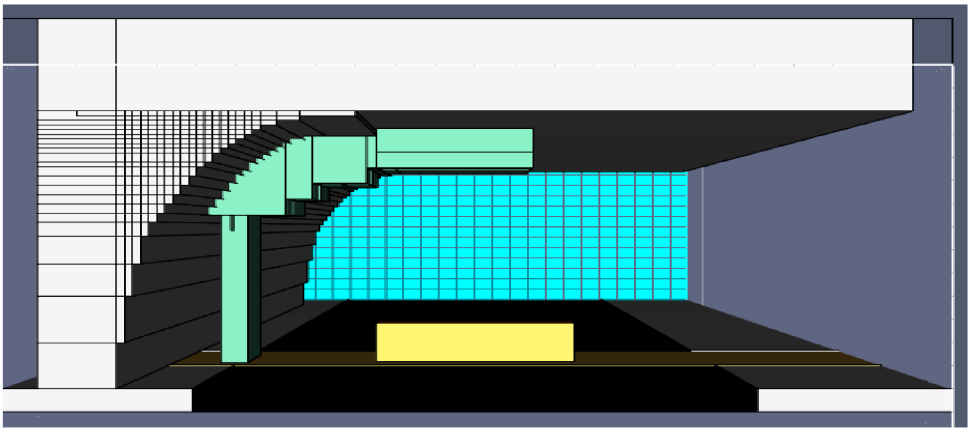

Figure 2. Step-rectangular meshes used to model tunnel ceiling surface.

In this work, our results have been evaluated by comparison against experiment values of [14]. Using grid cell sizes of 50, 60, and 70 cm, the results for radiation flux, at a ceiling 20 m downstream of the center of the fire, are shown in Figure 3. The trends of growth, maximum value, and decline were consistent with the experimental model. However, the levels of radiation 20 m downstream the fire were underestimated by approximately 40 and 85% for grid cells sizes of 50 and 70 cm, respectively.

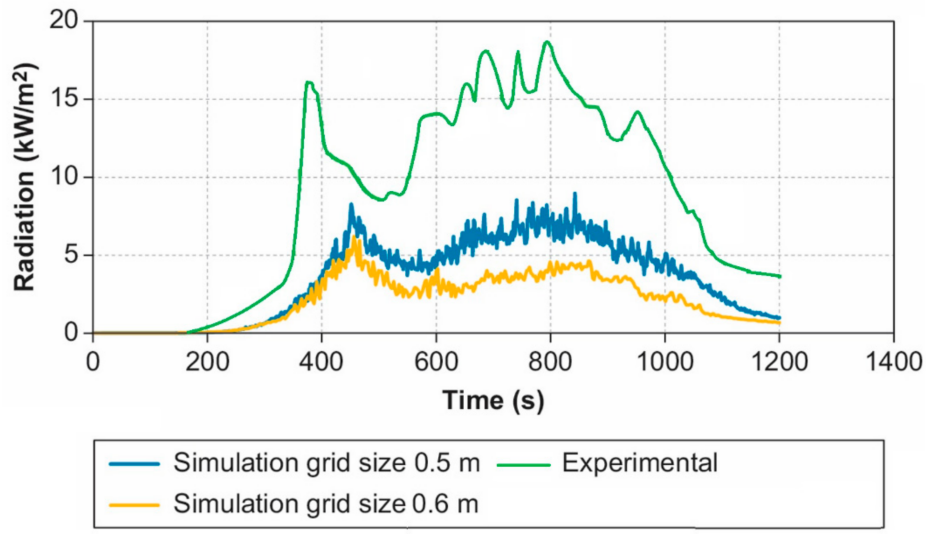

Figure 3. Radiation flux on the ceiling 20 m downstream of the source of fire.

However, Table 3 summarizes the precision and accuracy of the FDS simulations during 1200 s at each measuring point. A positive number indicates an overestimation, and an underestimation is indicated by a negative number. The simulations of radiation flux at ceiling 0 m downstream the fire show that all grid cell sizes highly underestimated the experimental data. In fact, by comparison to experimental data, the simulations showed that 12 and 22 kW/m^2 of maximal radiation was underestimated for 20 and 40 m downstream. In fact, the concentration of smoke, which is another input parameter controlled by FDS users, controls radiation, in part. This results in some confusion.

Table 3. Comparison between maximum simulated and experimental values of radiation flux.

Distance from Fire (m)	Measurements Placed on	Difference Estimating Maximum Radiation Level		Relative Difference Estimating Maximum Radiation Level (%)	
		Grid Cell Size (m)		Grid Cell Size (m)	
		0.5	0.6	0.5	0.6
0	Ceiling	−332.61	−376.42	−84.23	−96.05
20	Celling	−11.45	−88.24	−68.89	−82.50
40	Ceiling	−22.42	−11.91	−18.52	−63.61

Figure 4 shows an overestimation of the oxygen concentration 458 m downstream of the fire. This figure also prove that the oxygen concentration was uniform throughout the cross section. Trends were properly simulated, but the actual values of concentrations were not. This may be linked to the underestimated temperatures and levels of radiation near the fire, which may indicate lower heat production and consumption of oxygen. The underestimation of the temperature and radiation near the fire may indicate that the simulation fire was not as big as the actual fire. This may be the reason for the lower oxygen concentrations during the experiment.

Table 4 illustrates the grid cell sizes sensibility for oxygen concentration during 1200 s. A positive number indicates overstimulation, and an underestimation is indicated by a negative number. At the three measurement heights, the differences between measured and simulated levels were quite similar. While the maximum oxygen concentration was highly overestimated, by approximately 28%, the average difference between the simulation and the experimental results does not exceed 7%.

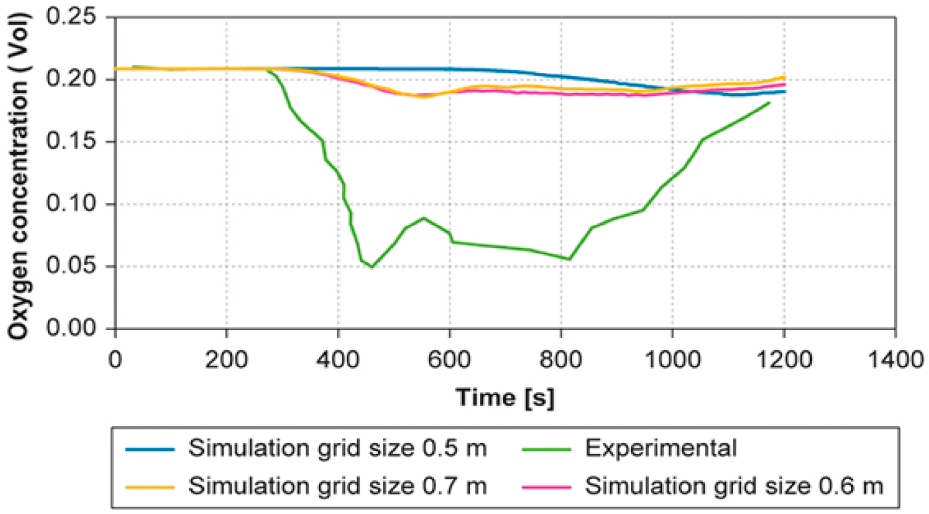

Figure 4. Oxygen concentration, 458 m downstream, 0.7 m above the road surface.

Table 4. Comparison between minimum simulated and experimental values of oxygen concentration.

Distance from Fire (m)	Height Above Road Surface (m)	Difference Estimating Minimum Oxygen Concentration			
		Grid Cell Size			
		50 cm		60 cm	
		mol/mol	%	mol/mol	%
458	5.1	13.81	27.92%	13.78	27.84%
458	2.9	13.82	27.94%	13.77	27.85%
458	0.7	13.818	27.93%	13.78	27.84%

Figure 5 and Table 5 show the results of the simulated and the measured air velocities in the tunnel 458 m downstream from the center of the flame at distinct heights. The results generally show convergence among all scenarios of grids of 0.5, 0.6, and 0.7 m because the air velocity in all cross-sectional zones is reasonably uniform, but a slight increase in air velocity occurs as the height decreases.

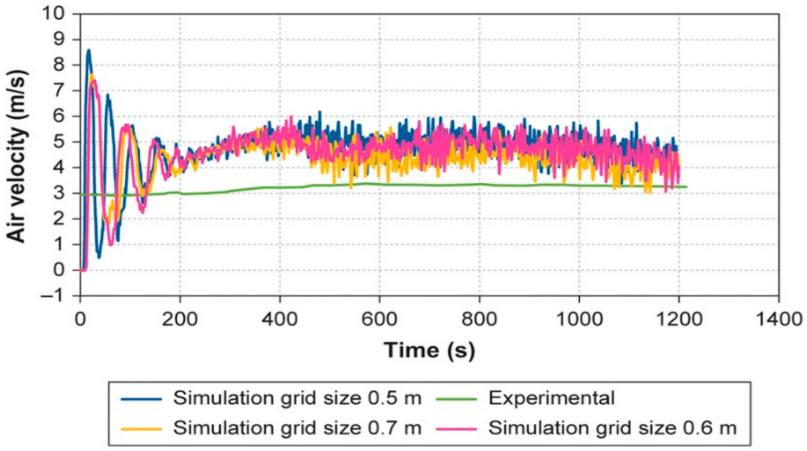

Figure 5. Air velocity, 458 m downstream, 2.9 m above road surface.

Table 5. Comparison between simulated and experimental values of air velocity.

Distance from Fire (m)	Grid Cell Size (cm)	Height above Road Surface (m)	Difference of Maximum Air Velocity		Difference of the Averaged Amount of Air Velocity	
			(m/s)	%	(m/s)	%
458	50	2.9	5.19	60.6	4.72	67.27
458	60	2.9	4.03	54.38	1.44	45.43
458	70	2.9	4.25	55.68	1.15	36.32

Table 6 prove that the temperature immediately above the fire was highly underestimated by approximately 360 °C. Figure 6 shows the same pattern as in the previous one, but the variation is less evident. The discrepancy during the trial between the top and the bottom measuring points was approximately 20 °C; however, during the simulation, there was almost no difference. Results indicate that the entire cross section has a continuous environment, rather than there being two layers: a warmer smoke layer and cooler layer of air. The temperatures were minimized for most of the measuring points around the fire (0–100 m downstream). Temperatures farther out, 250–350 m, were measured more precisely.

Table 6. Difference estimating temperature, averaged over first 1200 s.

Distance from Fire (m)	Height above Road Surface (m)	Difference Estimating Temperature Averaged over First 1200 s (°C)
0	5.7	−359.18
20	5.7	24.47
40	5.7	−158.43
100	5.7	−80.72
100	1.8	−71.94
250	5.7	−7.45
250	1.8	5.93
350	5.7	14.33
458	5.7	19.55

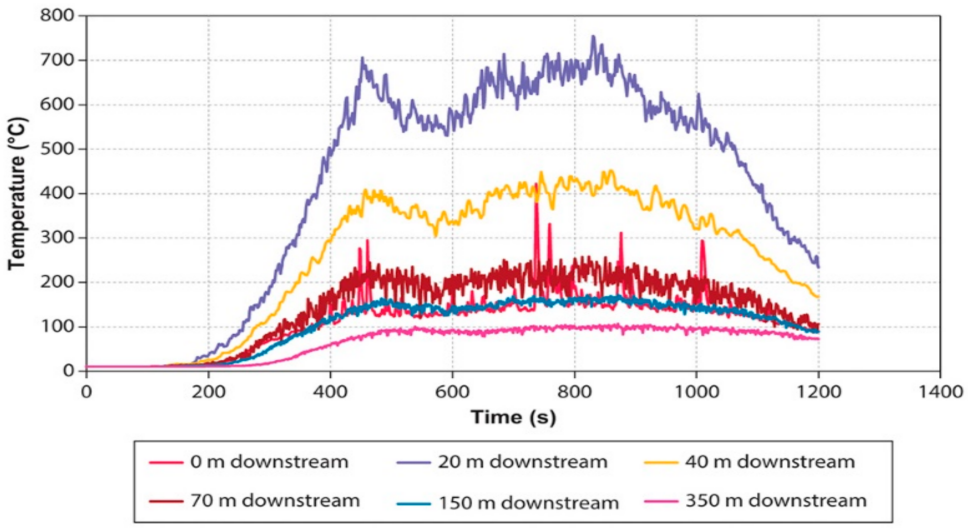

Figure 6. Gas temperature, 50 cm below the celling.

While the accuracy requirement of [19] has been verified, i.e., the dimensionless parameter D^*/dx = 10.28 has been chosen between 4 and 16, the trend in different result'

figures is that the measurements closest to the fire were underestimated or overestimated, and the results further away from the fire show an increasing accuracy, with an increasing distance. In fact, using more finer meshes, same conclusions have been proved by Le et al. [25] and Kim [26]. Le et al. [25] mentioned that their simulation results correlate well with the experimental measurements, especially from 10 m to 150 m downstream of the fire. However, the ceiling gas temperatures at 250 m and 350 m downstream were underestimated approximately 30% in the peak period. Additionally, they showed that the ceiling gas temperature is overestimated upstream of the fire. They explain that the back-layering length of a large tunnel fire could be overestimated using FDS. Additionally, the gas temperatures above the fire are overestimated in the peak period. This may appear from the difference in the fuel configuration, that is, the fuel involved of solid fuels in experimental test T1 of [14], but with gas burners in the simulation. In addition, based on the study of Kim [26] where same tunnel test T4 of [14] has been investigated, FDS simulated temperatures and flow velocities showing 30~40% discrepancies from those of the measured values. While a grid sensitivity analyses (30 cm, 48 cm, and 60 cm) were evaluated, the results proved that FDS have limitations in tunnel fires, which impact the smoke layer calculation at the upstream zone of the fire. Therefore, the author recommends that the simulations should include baroclinic torque which will help the mixing of the backlayer and forced ventilation flow, allowing less backflow propagation [26].

Our results proved the same above recommendations. In fact, in real test T4, 600 corrugated paper cartons with interiors (600 mm × 400 mm × 500 mm), 15% of total mass of unexpanded polystyrene (PS) cups (18,000 cups), 40 wood pallets (1200 × 1000 × 150 mm), and 10 m^2 polyester tarpaulin have been considered. In our simulations, the fire source has been replaced by a surface of 30 m^2 of diesel. Moreover, finer meshes can reduce the relative errors but the large discrepancies from those of the experiment values will persist as proved in [25,26]. In addition, the CPU time will be very high. In fact, using a personal computer (CPU of 2.6 GHz and a RAM of 3 GHz), the CPU run time was approximately 2.8, 6.3, and 10.6 days, when the grid size is 70, 60 and 50 cm, respectively. These significant errors can be explained by the model limitations which include the followings:

- FDS smoke layer prediction exposes concerns about extensive backflow in the FDS results, which occur when the inflow velocity at the boundary is slightly reduced. The resulting flow constriction causes the simulated tunnel fire conditions to deviate from those of the actual test.
- Rectilinear geometry: In our simulation the curved tunnel' surface has been modeled by rectangular grids. Thus, the efficiency of our results is due to the limitation of a rectangular grid cells. Therefore, new techniques are recommended to be implemented to reduce the effects.
- Combustion: FDS uses a mixture fraction combustion model. This model assumes that the reaction of fuel and oxygen is infinitely fast, and that the combustion is mixing controlled. For over-ventilated fires, this is a correct assumption. Combustion during under ventilated conditions and when a suppression agent is used, uncertainty increases since this is an area which needs more research.
- Radiation: To solve radiation methods like those used for convection are applied, finite volume methods. Because of simplifications used for combustion, the chosen chemical composition of the fuel and the soot yield can affect the absorption and emission of thermal radiation. Another simplification is that the radiative heat transport is discretized in 100 solid angles [19]. This can affect the distribution of radiant energy further away from the fire. This can be solved by increasing the number of angles, but this increases the computational time as well.

It is noted that, using Green–Lindsay thermoelasticity, a new form of energy equation and the paradox of the conduction of the heat proposed by Marin et al. [27]. This model can be considered as a proposed solution for zones far from the source of the fire where the temperature is low. In addition, general recommendations for more precise FDS simulations on tunnel fires with forced longitudinal ventilation can be developed. Several methods

were used to reduce the backflow: increasing the forced ventilation velocity near the ceiling, removing unwanted eddies near the stair-stepped ceiling, changing the flow slip condition near the ceiling, and restoring the baroclinic torque [26].

3.2. Study of fire in Makkah's King Abdulaziz Road Tunnel

The FDS results of fire tests in Makkah's King Abdulaziz Road Tunnel are discussed in this section. This tunnel is a highly crowded area during the Hajj season (Figure 7). The tunnel is in Ajyad district which is at the entrance to the holy Masjid al-Haram; hence, a fire in this tunnel could result in extensive loss of life and property. The road tunnel is 1198 m long, 6 m high, and 9 m wide, with a cross section of approximately 50 m^2 [16]. The fire was placed on a flat surface with an area of 20 m^2 and a height of 3.5 m at 1 m above the road surface. The geometry and structural features of this tunnel are similar to those of the Runehamar tunnel; therefore, the physical properties of the same materials were used in this study. The original values used in this section represent the same parameters used above.

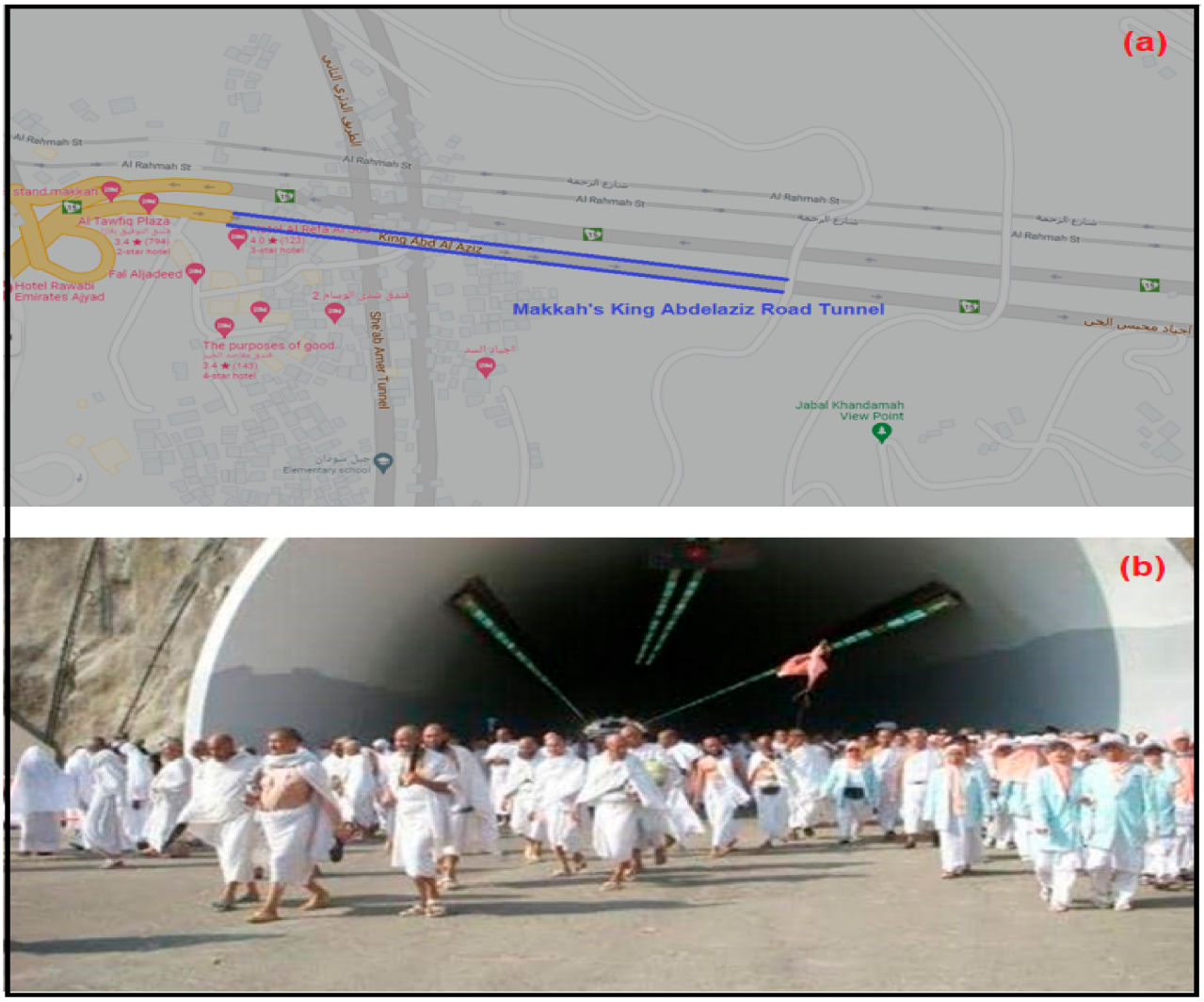

Figure 7. Makkah's King Abdelaziz Road Tunnel: (**a**) location and (**b**) its dense crowd during Hajj season.

To observe the temperature behavior within the tunnel clearly, the results were obtained at 100-, 350-, 450-, and 950-s intervals (Figure 8). The temperature scale selected was a range of 70 °C–350 °C for plots, comparing temperatures at various intervals. The fire spreads over time, and the temperature in the tunnel rises.

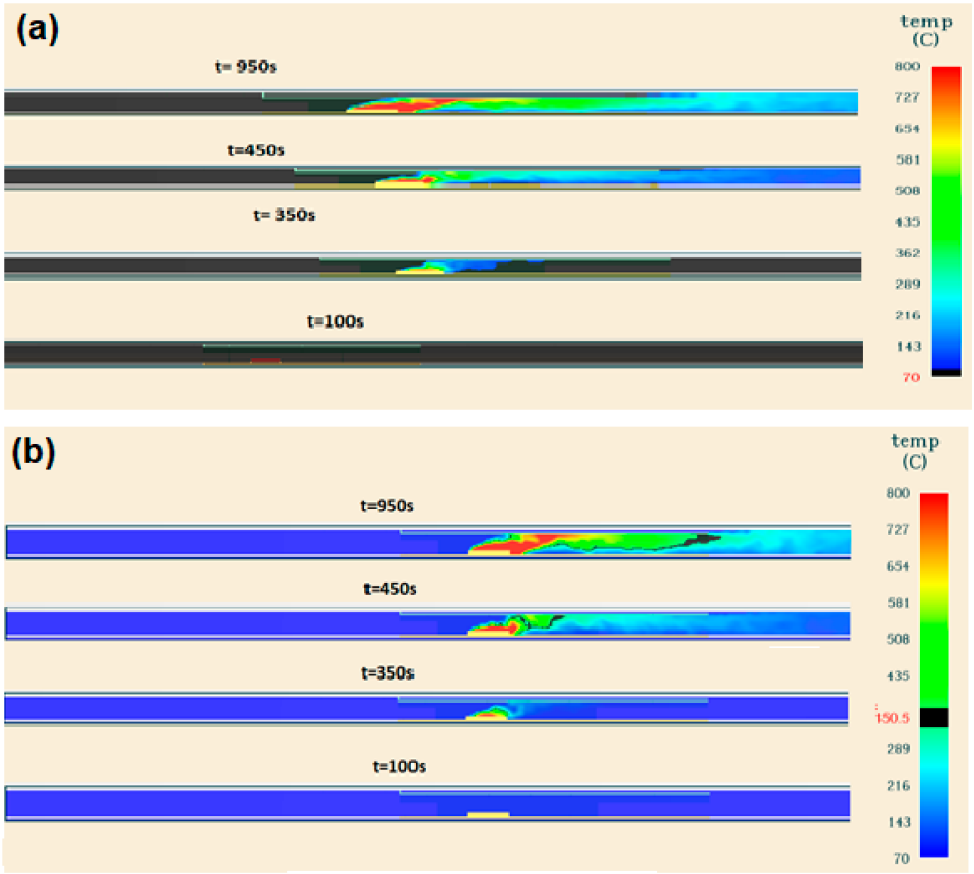

Figure 8. Contour plots of gas temperature with t = 100, 250, 350, 450, and 950 s for (**a**) T = 70 and (**b**) 350.5 °C.

3.2.1. Effects of HRRPUA

To study the influence of the of HRRPUA in tunnel fire simulation, ±15% of original value has been tested. The increase of HRRPUA produces a larger fire if the fire area is maintained unchanged. Therefore, all results were as expected. While gas temperature, radiation flux, CO and CO_2 concentrations, and air velocity increased, the oxygen concentration decreased (Table 7). For radiation flux at ceiling, an increase ratio of approximately 54% and decrease of approximately 33% have been obtained for changes of HRRPUA of ±15%, and −15%, respectively. Furthermore, the amount of heat emitted increases, and the concentration of the combustion products CO and CO_2 increase by approximately 10–16%, consuming more oxygen. The increase of HRRPUA makes an increased heat production, warmer fire, and decrease of the temperature (Figure 9). However, if this parameter is reduced by −15%, smaller heat production and cooler fire have been produced.

3.2.2. Effects of Soot Yield

Figure 10 shows the contour plots of soot yield at t = 250 and 950 s. The fire spreads over time, and visibility in the tunnel decreases. The effect of soot yield change on temperature, HRR, oxygen, CO and CO^2 concentrations, and air velocity are shown in Table 8. This table indicates that when the soot yield decreases by 25%, the temperature and HRR decrease by approximately 29% and 41%, respectively. For the CO and CO_2 concentrations, a decrease was observed when the soot yield decreased. However, the change was almost unaffected by the concentration of oxygen and air velocity.

Table 7. Effects of HRRPUA.

Parameter	Original Value	+15%	Difference Ratio (%)	−15%	Difference Ratio (%)
Temperature (°C)	50.27	55.90	11.19	46.20	−8.11
Radiation flux (W/m^2)	−10,407.18	−23,096.42	54.94	−15,308.88	−32.02
Oxygen concentration (mol/mol) × 10^{-2}	19.86	19.61	−1.25	20.02	0.87
CO concentration (mol/mol) × 10^{-5}	13.01	15.89	22.13	10.87	−25.57
CO_2 concentration (mol/mol) × 10^{-5}	8.64	10.41	20.45	7.25	−16.08
Air velocity (m/s)	3.52	0.29	4.44	3.51	−0.86

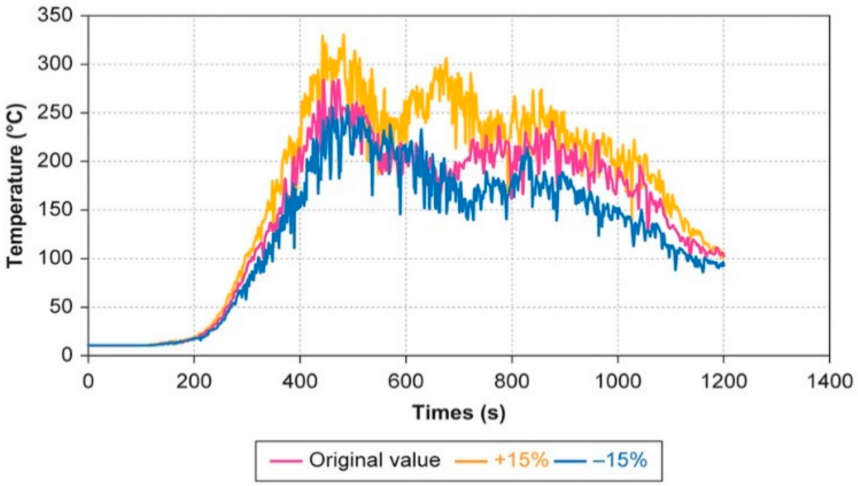

Figure 9. Effects of HRRPUA on gas temperature 70 m below the ceiling.

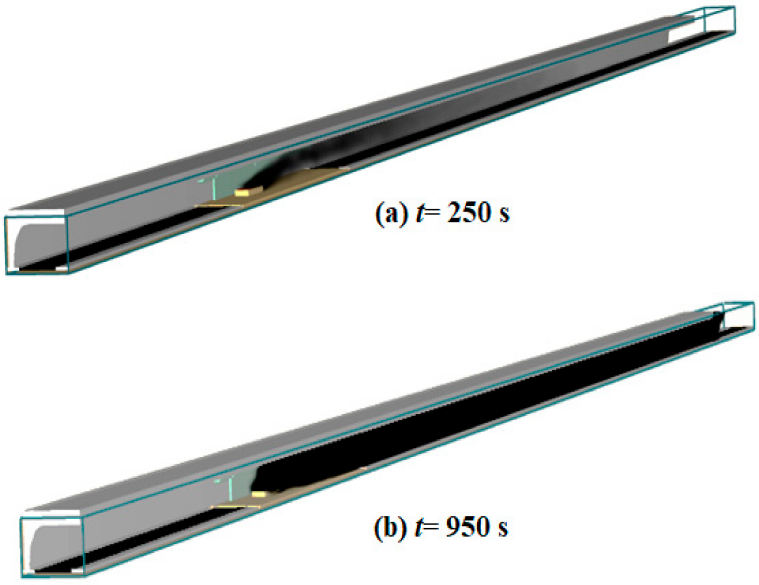

Figure 10. Contour plots of soot yield at (**a**) t = 250 and (**b**) 950 s.

Table 8. Effects of soot yield.

Parameter	Soot Yield Change				
	Original Value	**+25%**	**Difference Ratio (%)**	**−25%**	**Difference Ratio (%)**
Temperature (°C)	50.27	55.40	9.26	56.76	−12.91
HRR (kW)	22,722.81	41,404.86	45.12	40,705.8	44.18
Oxygen concentration (mol/mol) × 10^{-2}	19.84	19.71	−0.65	−19.69	−0.76
CO concentration (mol/mol) × 10^{-5}	13.01	15.05	15.68	−14.73	−12.57
CO_2 concentration (mol/mol) × 10^{-5}	8.64	9.61	11.22	−9.95	−15.16
Air velocity	3.52	3.71	5.39	3.69	−4.65

3.2.3. Effects of CO Yield

The change in the CO yield generally influenced only the CO concentration. Figure 11 shows the CO concentration 458 m downfield of the source fire, 5.1 m above the road surface. This figure shows that the increase of CO yield, by 10% of the original value, produced higher CO levels and lower CO yields, which produced lower CO levels.

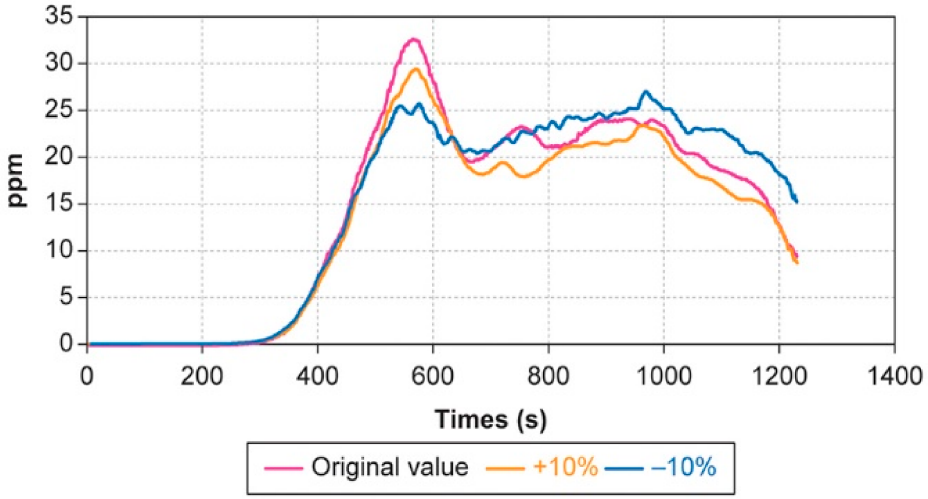

Figure 11. CO yield effects on CO concentration, 458 m downfield and 5.1 m above road surface.

Table 9 presents the effect of changing the CO yield of the fire on different parameters. The CO yield significantly affects the CO concentration, but it is negligible for the other studied parameters. Changing the CO yield by ±10% affects the CO concentration by approximately ±60 % (Table 9).

However, its effects on temperature and air velocity are moderate (Figures 12 and 13).

In addition, the combustion heat generally determines which energy is emitted to burn the fuel per unit weight. Both parameters, CO and soot yield, which depend on combustion heat, are affected. Therefore, the change of CO yield changes the heat of combustion by ±10% (Figure 14).

Table 9. Effects of CO yield.

Parameter	CO Yield Change				
	Original Value	+10%	Difference Ratio (%)	−10%	Difference Ratio (%)
Temperature (°C)	50.27	50.66	0.78	55.07	−8.73
Oxygen concentration (mol/mol) × 10^{-2}	19.84	19.86	0.09	−19.59	−1.27
CO concentration (mol/mol) × 10^{-5}	13.01	14.273	9.68	−14.73	−11.15
CO2 concentration (mol/mol) × 10^{-5}	8.64	11	27.19	−5.73	−33.68
Air velocity (m/s)	3.52	3.53	0.47	−3.31	−8.61
HRR (kW)	20,993.78	36,620.56	42.67	40,894.22	48.66

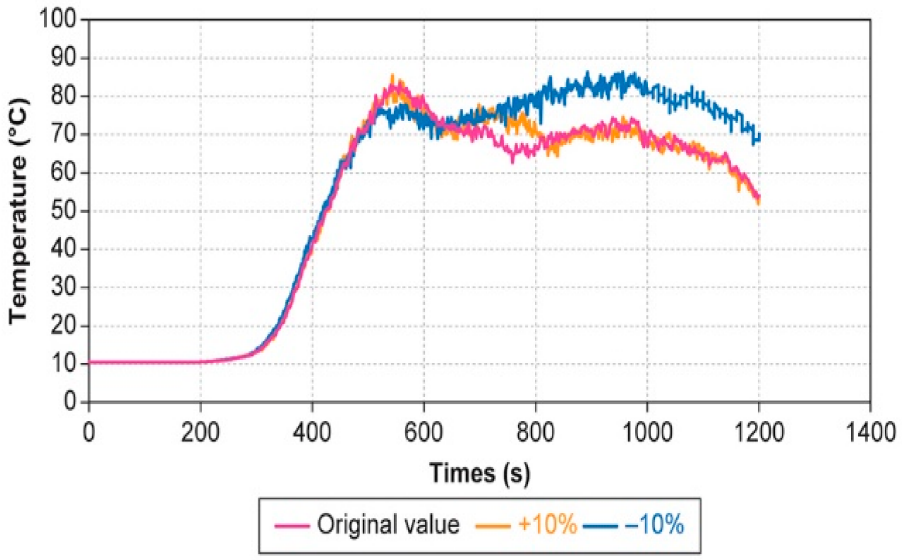

Figure 12. CO yield effects on gas temperature, 458 m downstream and 5.1 m above road surface.

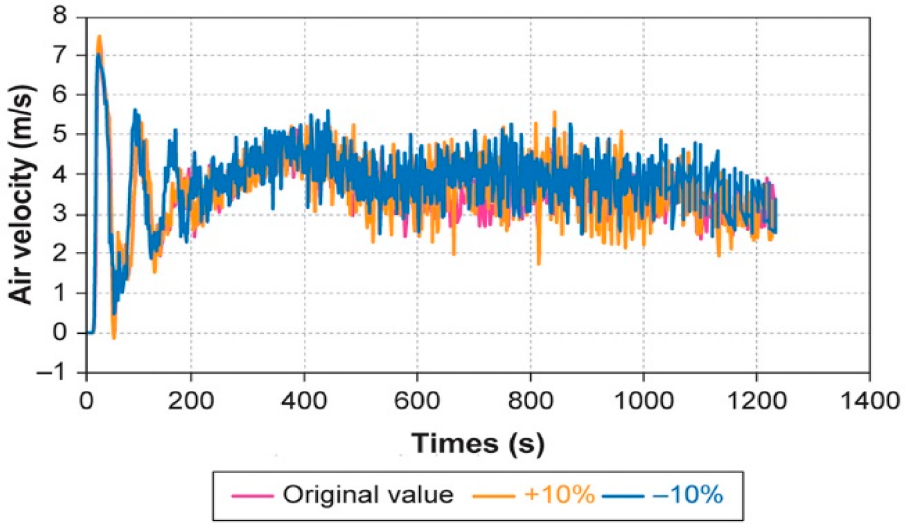

Figure 13. CO yield effects on air velocity.

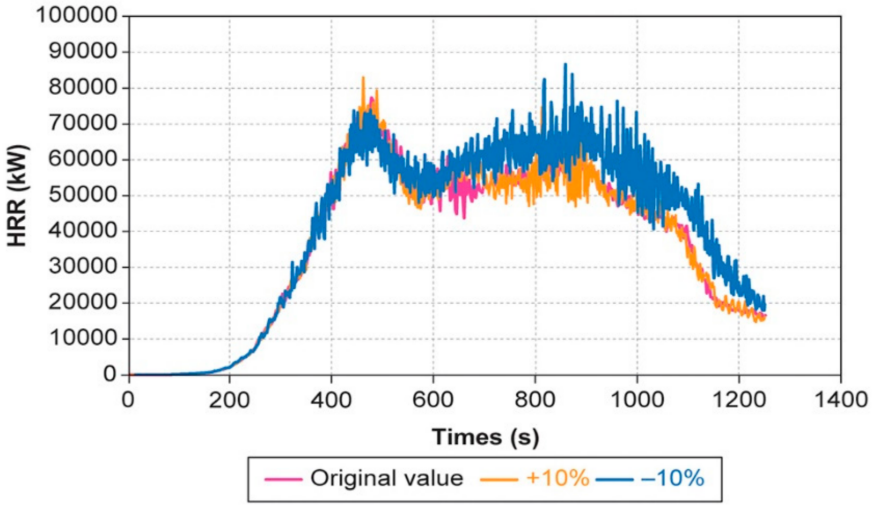

Figure 14. CO yield effects on HRR.

4. Conclusions

In the present work, a parametric study of fire simulation in the Makkah King Abdulaziz Road Tunnel was investigated. The effects of the HRRPUA and soot yield on the gas temperature, radiation, concentrations of the combustion products CO and CO_2, and air velocity were analyzed, using the FDS. The results show that (1) when the HRRPUA is increased by 15%, the radiation increases by approximately 54%; (2) the decrease of HRRPUA by 15% decreases the radiation by approximately 32%; and (3) the change of the soot yield affects all parameters, except oxygen concentration and air velocity. Because tunnel fires have severe impacts on various aspects of people's lives, it is crucial to address tunnel safety. In addition, this issue could extend to influencing the tunnel structure, which requires comprehensive research. Moreover, based on the validation part, FDS simulations, showing large discrepancies from those of the experiment values, which proved that FDS have limitations in tunnel fires, which affect the smoke layer prediction at the upstream region of the fire. Therefore, the users or researchers should be careful and concerned about these weaknesses when using FDS to simulate tunnel fires or make engineering decisions based on the model computations to optioned suitable safety means for tunnel fires.

Author Contributions: Conceptualization, K.G.; methodology, K.G., M.O., A.B. and S.M.M.; software, K.G., A.A.A. and O.S.B.; validation, K.G., A.A.A. and O.S.B.; formal analysis, K.G., A.A.A., O.S.B. and M.O.; investigation, K.G., A.A.A., O.S.B., M.O., A.B. and S.M.M.; resources, K.G., A.A.A., O.S.B. and S.M.M.; data curation, K.G. and A.B.; writing—original draft preparation, K.G., A.A.A., O.S.B., M.O., A.B. and S.M.M.; writing—review and editing, K.G., A.A.A., O.S.B., M.O., A.B. and S.M.M.; visualization, K.G., A.A.A. and O.S.B.; supervision, K.G., A.A.A., O.S.B., M.O., A.B. and S.M.M.; project administration, K.G.; funding acquisition, K.G. All authors have read and agreed to the published version of the manuscript.

Funding: This research received no external funding.

Data Availability Statement: Not applicable.

Acknowledgments: The authors would like to thank the Deanship of Scientific Research at Umm Al-Qura University for supporting this work by grant code: 19-ENG-1-01-0013.

Conflicts of Interest: The authors declare no conflict of interest.

References

1. Lapointe, C.; Wimer, N.T.; Simons-Wellin, S.; Glusman, J.F.; Rieker, G.B.; Hamlington, P.E. Efficient simulations of propagating flames and fire suppression optimization using adaptive mesh refinement. *Fluids* **2021**, *6*, 323. [CrossRef]
2. Kodakoglu, F.; Demir, S.; Valiev, D.; Akkerman, V. Analysis of gaseous and gaseous-dusty, premixed flame propagation in Obstructed passages with tightly placed obstacles. *Fluids* **2020**, *5*, 115. [CrossRef]

3. Li, L.; Zhu, D.; Gao, Z.; Xu, P.; Zhang, W. A study on longitudinal distribution of temperature rise and carbon monoxide concentration in tunnel fires with one opening portal. *Case Stud. Therm. Eng.* **2021**, *28*, 101535. [CrossRef]
4. Xu, X.; Zhu, G.; Zhang, X.; Chai, G.; Chu, T. Numerical study on temperature distribution of tunnel structure in fires. *Case Stud. Therm. Eng.* **2021**, *21*, 100874. [CrossRef]
5. Halawa, T.; Safwat, H. Fire-smoke control strategies in road tunnels: The effectiveness of solid barriers. *Case Stud. Therm. Eng.* **2021**, *27*, 101260. [CrossRef]
6. Gao, Y.; Zhu, G.; Gu, S.; Tao, H.; Zhao, Y. Experimental and numerical studies on ceiling maximum smoke temperature and longitudinal decay in a horseshoe shaped tunnel fire. *Case Stud. Therm. Eng.* **2018**, *12*, 134–142. [CrossRef]
7. Fragkopoulou, M. Road Tunnel Fire Safety: Determining the Effect of the Performance of Technological Systems for Fire Detection on Fire Detection Time and on the Total Evacuation Time. Master's Thesis, Department of Building Engineering, TU Delft, Delft, The Netherlands, 2016.
8. Peacock, R.D.; Walter, W.; Jones, W.; Reneke, P.A.; Forney, G.P. *CFAST–Consolidated Model of Fire Growth and Smoke Transport (Version 6)*; special publication 1041; NIST: Gaithersburg, MD, USA, 2005.
9. Wu, C.A. System Architecture for the Integration of Smoke Propagation Simulation, Evacuation Simulation, and Building Information Modelling. Ph.D. Thesis, Texas A&M University, College Station, TX, USA, 2017.
10. Floyd, J.E. Evaluation of the Predictive Capabilities of Current Computational Methods for Fire Simulation Using the HDR T51 and T52 Tests with a Focus on Performance-Based Fire Codes. Ph.D. Thesis, University of Maryland, College Park, MD, USA, 2000.
11. Luo, J.; Xu, Z.; Li, F.; Zhao, J. Effect of vehicular blocking scene on smoke spread in the longitudinal ventilated tunnel fire. *Case Stud. Therm. Eng.* **2019**, *14*, 100495. [CrossRef]
12. Wang, X. Fire Dynamics Simulator (FDS) Pyrolysis Model Analysis of Heavy Goods Vehicle Fires in Road Tunnels. Ph.D. Thesis, University of Canterbury, Christchurch, New Zealand, 2017.
13. Bilge, M.İ. CFD Simulation of Train Fire in the İstanbul Metro Tunnel. Master's Thesis, Middle East Technical University, Ankara, Turkey, 2018.
14. Ingason, H.; Li, Y.Z.; Lönnermark, A. *Tunnel Fire Dynamics*; Springer: New York, NY, USA, 2014.
15. Keita, T.; Futoshi, K.; Khalid, T.; Moinuddin, A.M. Combustion efficiency during fires in tunnels with natural ventilation by vitiated air including descending smoke. *Fire Saf. J.* **2021**, *120*, 103093. [CrossRef]
16. Sargininsaat. Available online: https://sargininsaat.com/en/?page_id=198 (accessed on 15 November 2021).
17. Li, Y.Z.; Bo, L.; Ingason, H. Study of critical velocity and backlayering length in longitudinally ventilated tunnel fires. *Fire Saf. J.* **2010**, *45*, 361–370. [CrossRef]
18. Blazek, J. *Computational Fluid Dynamics: Principles and Applications*; Butterworth-Heinemann, Elsevier Ltd.: Oxford, UK, 2015. [CrossRef]
19. McGrattan, K.; Hostikka, S.; McDermott, R.; Floyd, J.; Weinschenk, C.; Overholt, K. *Fire Dynamics Simulator Technical Reference Guide, Volume 3: Validation*; special publication 1018-3; NIST: Gaithersburg, MD, USA, 2017.
20. Lönnermark, A.; Claesson, A.; Lindström, J.; Li, Y.Z.; Kumm, M.; Ingason, H. *Full-Scale Fire Tests with a Commuter Train in a Tunnel*; Fire Technology SP Report: 2012:05; SP Technical Research Institute of Sweden: Borås, Sweden, 2012; ISSN 0284-5172.
21. Carvel, R.O.; Beard, A.N.; Jowitt, P.W.; Drysdale, D.D. Variation of heat release rate with forced longitudinal ventilation for vehicle fires in tunnels. *Fire Saf. J.* **2001**, *31*, 569–596. [CrossRef]
22. Carvel, R.O.; Beard, A.N.; Jowitt, P.W.; Drysdale, D.D. The influence of tunnel geometry and ventilation on the heat release rate of a fire. *Fire Technol.* **2004**, *40*, 5–26. [CrossRef]
23. Ingason, H.; Li, Y.Z. Model scale tunnel fire tests with longitudinal ventilation. *Fire Saf. J.* **2010**, *45*, 371–384. [CrossRef]
24. Guedri, K.; Borjini, M.N.; Jeguirum, M.; Brilhac, J.-F.; Said, R. Numerical study of radiative heat transfer effects on a complex configuration of rack storage fire. *Energy* **2011**, *36*, 2984–2996. [CrossRef]
25. Li, Y.Z.; Ingason, H.; Lönnermark, A. Numerical simulation of Runehammer tunnel fire tests. In Proceedings of the 6th International Symposium "Tunnel Safety and Ventilation", Graz, Austria, 23–25 April 2012; Sturm, P.J., Minarik, S., Eds.; Volume 95, pp. 203–210.
26. Kim, E. A Study of Pulsation in Runehammer Tunnel Fire Tests with Forced Longitudianal Ventilation. Ph.D. Thesis, Worcester Polytechnic Institute (WPI), Texas A&M University, Dallas, TX, USA, 2006.
27. Marin, M.; Craciun, E.M.; Pop, N. Some results in green–lindsay thermoelasticity of bodies with dipolar structure. *Mathematics* **2020**, *8*, 497. [CrossRef]